

LOW EMITTANCE IMMERSSED AND NON-IMMERSSED FOILLESS DIODES FOR HIGH CURRENT ELECTRON LINACS*

M. G. Mazarakis, J. W. Poukey, S. L. Shope, D. E. Hasti,
D. L. Smith, M. D. Haworth[†], C. A. Frost,
G. T. Leifeste and J. S. Wagner

Sandia National Laboratories, Albuquerque, NM 87185

[†]Science Applications International Corporation, Albuquerque, NM 87106

ABSTRACT

A low emittance immersed foilless diode injector was designed and built for the upgraded RADLAC-II accelerator. The design is for a 5-MV, 40-kA annular beam with a 9-mm outer radius. A conical cathode field shaper eliminates the previously observed large cathode shank losses. The non-immersed foilless diode approach was utilized in the design of the Sandia recirculating linear accelerator (RLA) injector. A low energy design (~1.7 MV) and high energy (4 MV) design were carried out in conjunction with a solenoidal vacuum beam transport and injection system.

INTRODUCTION

Foilless diode electron sources are the most appropriate for very high current, high energy linear accelerator. They produce well defined 10 - 100-kA beams that can be easily transported and further accelerated through the post-accelerating gaps of the device. The beam transport can be accomplished either with magnetic lenses and solenoids or with ionized plasma channels operating in the Ion Focusing Regime (IFR).⁽¹⁾

We have investigated two types of foilless diodes: a magnetically immersed and a non-immersed configuration. The non-immersed diodes are ideally fit for the lower end of the beam current range of interest. Both approaches can produce very low temperature beams with transverse velocities of the order of $\beta_{\perp} = 0.05$. The immersed diodes are preferred for applications where the beam either does not exit the solenoidal magnetic field such as free electron lasers, x-ray production devices, microwave generators, etc., or is extracted from the accelerator after it has acquired high energies (~20 MV). The reason is that these diodes produce beams with considerable canonical angular momentum (P_{θ}) which spin quite fast once out of the magnetic field in which they were generated. Consequently, after extraction, an additional term is quadratically added to the transverse velocity equal to the angular velocity v_{θ} . The non-immersed foilless diode does not have the canonical angular momentum limitations; however, because of space charge in the A-K gap region, it cannot produce larger than 20-kA laminar beams with reasonable size radii (5-10 cm). The beam in the RADLAC-II⁽²⁾ accelerator is magnetically transported and accelerated up to 20 MV before being extracted from the 20-KG solenoidal magnetic field. On the other hand, in our Recirculating Linear Accelerator (RLA)⁽¹⁾ the beam is extracted from the diode injector at energies between 1.5 - 4 MV and is then injected into a closed geometry racetrack-shaped beam containment vessel similar to a conventional "storage ring." There the beam is recirculated many times through the post-accelerating gaps with the aid of a non-magnetic IFR transport channel. Hence, for the RADLAC-II

accelerator, we selected an immersed foilless diode while for the RLA, the non-immersed diode appears to be a more appropriate choice.

In this paper, we report a new immersed foilless diode for the upgraded RADLAC-II⁽³⁾ accelerator and a non-immersed foilless diode injector for the Sandia Recirculating Linac.

The New RADLAC-II Foilless Diode Injector Design

Figure 1 shows the RADLAC-II injector cavity where the foilless diode and both the cathode and anode field shapers are located. The beam current is monitored by a Rogowski coil located 1.4-m downstream from the A-K gap of the foilless diode. The total current emitted by the cathode shank and by the cathode field shaper (Fig. 1) is measured by a larger Rogowski monitor surrounding the base of the field shaper inside the injector cavity.

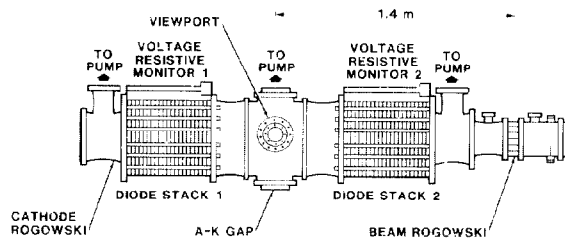


Fig. 1. RADLAC-II injector cavity.

A conical design was chosen for the new cathode field shaper which starts at the cathode end plate with a 10-cm diameter cylinder and tapers off smoothly at the cathode tip. The half angle of the cone is 4° and the radius of the conical surface as a function of the distance from cathode end plate is such that it can provide magnetic insulation against radial emission all along its length. The magnetic field at the A-K gap is 20 kG.

Some radial losses occur in a region where the magnetic insulation would be expected to fail if there were not a self-magnetic field B_{θ} . On the anode side of the region, magnetic insulation is obtained due to the guiding magnetic field B_z . Figure 2 shows the equipotential surfaces for the conical injector as

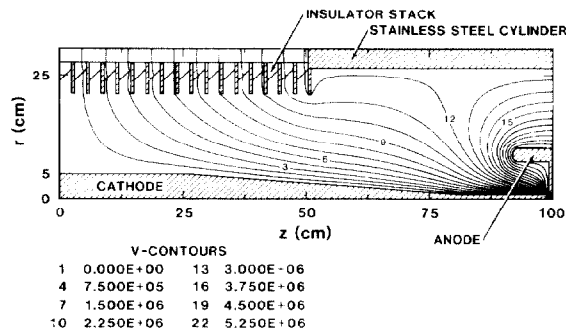


Fig. 2. Equipotential plot for the new conical field shaper.

*This work was supported by the U.S. Department of Energy under contract number DE-AC04-76DP00789, by DARPA/AFWL under Project Order AFWL86-154, and by the U.S. Navy SPAWAR under Space Task 145-SNL-1-9-1.

obtained by the JASON⁽⁴⁾ code, and Figure 3 gives the electron map for the new injector geometry. A new version of MAGIC⁽⁵⁾ which includes subroutines allowing space-charge limited emission from slanted conducting surfaces was utilized for these simulations. The shank current losses are 7.5%.

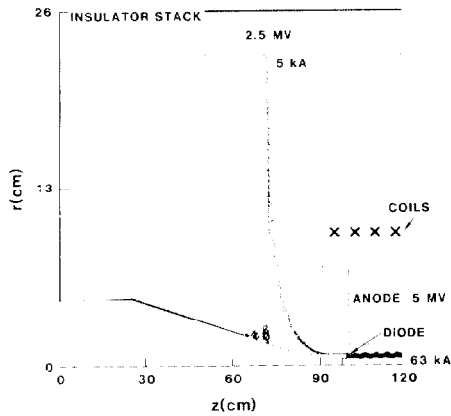


Fig. 3. Electron map for the new injector. The applied voltage to the A-K gap is 4.75 MV. All electron losses occur radially and account only for 5 kA of the 68 kA total shank current.

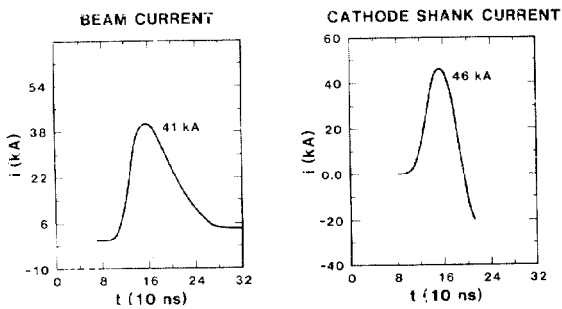


Fig. 4. Total shank and beam current for a 4.1-MV injector voltage. The shank current losses (=shank current minus beam current) are less than 11%.

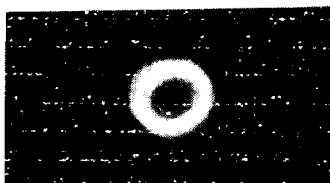


Fig. 5. Time-integrated pinhole photograph of the beam from the new injector. The slight ellipticity is due to a small parallax between the beam and camera axis.

The experimental results indicate good agreement between numerical simulation and measurements. The measured cathode shank current losses are only 5-11%. Beam currents range from 35 kA at 3.6 MV to 41 kA at 4.1 MV (Fig. 4). The cathode shank current for those shots was 37 kA and 45 kA. As shown by the time-integrated x-ray pinhole photograph (Fig. 5), the beam halo is eliminated and the beam is annular without any appreciable filling-in. From Figure 5, we estimate⁽⁶⁾ a $\beta_1=0.10$.

The superior beam quality produced by the injector has been further verified in the most recent experiments⁽⁷⁾. A very well defined ~40 kA annular beam was generated and transported through the first half of the upgraded RADLAC-II accelerator structure (~5 m downstream from the cathode tip) without any losses or beam quality deterioration. Actually the measured β_1 after the beam had been accelerated by the first two post-accelerating gaps was smaller than that at the injection point and of the order of $\beta_1 \approx 0.08$.

The RLA Non-Immersed Foilless Diode Injector and Beam Transport System

The present RLA configuration consists of a 1.7-MV isolated Blumlein injector⁽¹⁾ and one post-accelerating cavity with the accelerating gap located inside the IFR channel. The electron diode of the injector is outside the racetrack and ~1.5 m away. The beam cannot be transported from the injector to the racetrack with a straight IFR channel formed by the same low electron beam (LEEB) ionizing technique as the one utilized for the racetrack IFR. The solenoids of the two IFR channels would not be compatible at the intersection point. The foilless diode design presented here produces a very cold beam which can be magnetically transported into the injection area through a vacuum line with minimum beam temperature increase.

The diode design presented here incorporates the advantages of both a planar and an immersed foilless diode. It produces a fairly parallel laminar beam with small divergence as in the case of the planar diode (Fig. 6). The pinching effect of the anode foil is eliminated along with the canonical angular momentum term of an immersed foilless diode.

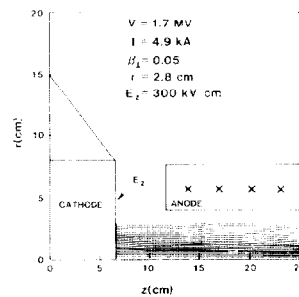


Fig. 6. Non-immersed foilless diodes can produce very cold beams.

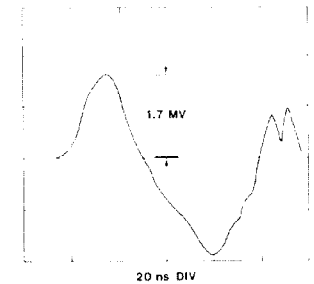


Fig. 7. Injector voltage as measured along the diode stack.

Close to the anode electrode, the beam encounters the magnetic field region of the transport system. The cathode is at zero magnetic field. The electric field at the cathode is kept as low as possible and at a right angle to the cathode surface ($E_r = 0$). The electron emission region is specified by an area covered with felt which starts undergoing explosive electron emission at as low an electric field as 60 kV/cm. The current density for these configurations scales as

$$j = \frac{3.52 \times 10^3}{d^2} \left[\gamma^{2/3} - 1 \right]^{3/2} \quad (1)$$

where $\gamma = eV/mc^2 + 1$. The A-K gap (d) is selected depending on the beam radius and total current required for each diode voltage.

In designing these diodes, we select first the approximate A-K gap and define the emitting area according to the scaling formula (1). Then we define

the shape of the electrodes using the JASON code.⁽⁴⁾ Finally, we use the code TRAJ⁽⁸⁾ to study the beam production and to design the magnetic transport system. Much care is taken in designing the cathode surfaces to avoid electric fields in excess of 200 kV/cm. However, since the voltage of the present injector is bi-polar (Fig. 7), attention is given to reducing the field on the anode electrode. Figure 8 is a design of the 1.7-MV diode with both cathode and anode electrode shapes optimized. Figure 9 shows the electron trajectories for the 1.7-MV case. Figure 10 shows the magnetic

field on axis generated by two solenoids and three focusing coils. It must be close to zero not only at the emitting surface of the cathode but also at the injection point in order to prevent any interference with IFR channel. Figure 11 presents a 4-MV, 10-kA design for our new RIA injector.

CONCLUSIONS

A new immersed and a non-immersed foilless diode injector has been recently designed and constructed respectively for the upgraded RADLAC II and the Recirculating Linear Accelerator (RLA). Creedon's model formalism⁽⁹⁾, the JASON code and the new version of MAGIC PIC code that includes the slant geometry package was extensively utilized for the immersed diode injector design. The design of the non-immersed diode and beam transport system is simpler, and only the JASON and the trajectory code TRAJ were necessary to simulate this diode.

The new RADLAC-II injector has been installed and very successfully operated. It met and in many instances exceeded all of our design goals. The previously observed excessive electron losses have been eliminated. The total measured shank current is only 5-10% higher than the 40-kA beam current. A high quality annular beam was generated with a $\beta|$ of 0.1 and normalized emittance equal to 0.8 rad-cm. This beam was injected into the RADLAC-II beam line and further accelerated by the first two post-accelerating gaps without losses or emittance increase.

The non-immersed foilless diode injector will be installed in our RLA and experimentally validated in a few weeks. We expect it to produce a very low temperature and emittance electron beam which will be transported in a vacuum beam pipe with no losses and minimum quality degradation. The elimination of the anode foils and of the previously utilized gas cell, wire zones and classical IFR, makes this injector attractive.

REFERENCES

1. S. L. Shope, et al., "Acceleration and Bending of a Relativistic Electron Beam on the Sandia Recirculating Linac," *Proc. IEEE Part. Accel. Conf.*, Washington, DC, March 1987, CH2387-9/87/0000-0908.
2. M. G. Mazarakis, et al., "RADLAC Accelerator Beam Experiments," *Proc. of the IEEE Part. Accel. Conf.*, Washington, DC, March 16-19, 1987, CH2387-9/87/0000-0908.
3. S. L. Shope, et al., "The Upgraded RADLAC-II Accelerator," *Proc. of the 1988 Linear Accel. Conf.*, Williamsburg, VA, October 3-7, 1988, to be published.
4. S. J. Sackett, "JASON-A Code for Solving General Electrostatics Problems User's Manual," LLL Report UCID-17814. Revised by M. L. Kiefer, Sandia National Laboratories, Albuquerque, NM (1984).
5. B. Goplen, et al., "Users Manual for MAGIC/Version-Sept. 1983, MRC/WDC-R/068," Mission Research Corp., Washington, DC, (1983)
6. D. E. Hasti, et al., "RADLAC-II Upgrade Injector Experiments," SNLA SAND88-1032, Albuquerque, NM (1988).
7. S. L. Shope, et al., "RADLAC-II Upgrade Experiments," this Conference.
8. J. W. Poukey, "Trajectory vs. PIC Methods on Diode Design," *Proc. of 12th Conf. on Numerical Simulations of Plasma*, San Francisco, CA, (9/87).
9. J. M. Creedon, *J. Appl. Phys.* **48**(3), 1070 (1977).

EQUIPOTENTIAL PLOT 1.7 MV ANODE VOLTAGE

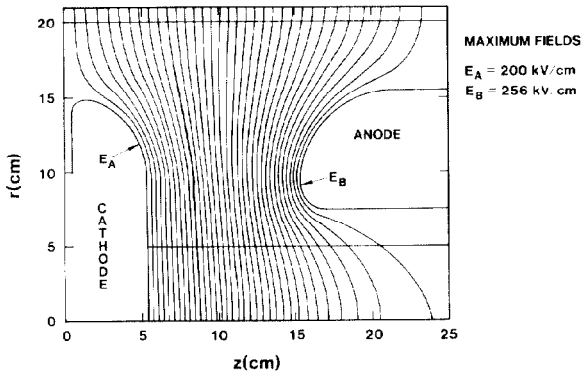


Fig. 8. Both the anode and cathode surface shapes are optimized for minimum electric field stresses.

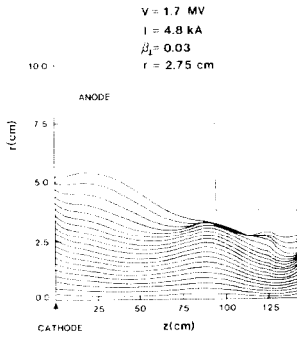


Fig. 9. Electron trajectories. The quoted transverse velocity and radius are at the exit foil (located at $z=146$ cm).

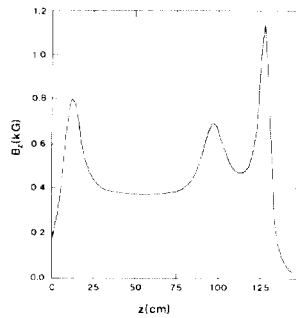


Fig. 10. The magnetic field B_z on axis.

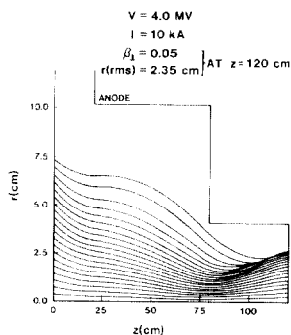


Fig. 11. Electron trajectories for a 4-MV beam.